

Localized electrochemical oxidation of p-GaAs(100) using atomic force microscopy with a carbon nanotube probe

This content has been downloaded from IOPscience. Please scroll down to see the full text.

2006 Nanotechnology 17 3838

(<http://iopscience.iop.org/0957-4484/17/15/039>)

View [the table of contents for this issue](#), or go to the [journal homepage](#) for more

Download details:

IP Address: 140.113.38.11

This content was downloaded on 26/04/2014 at 08:51

Please note that [terms and conditions apply](#).

Localized electrochemical oxidation of p-GaAs(100) using atomic force microscopy with a carbon nanotube probe

Wu-Ping Huang¹, Hung-Hsiang Cheng¹, Sheng-Rui Jian^{2,6},
Der-San Chuu², Jin-Yuan Hsieh³, Chih-Ming Lin⁴ and
Mu-Sheng Chiang⁵

¹ Graduate Institute of Electronics Engineering and Center for Condensed Matter Sciences, National Taiwan University, Taipei 106, Taiwan

² Department of Electrophysics, National Chiao Tung University, Hsinchu 300, Taiwan

³ Department of Mechanical Engineering, Ming Hsin University of Science and Technology, Hsinchu 30401, Taiwan

⁴ Department of Applied Science, National Hsinchu University of Education, Hsinchu 30014, Taiwan

⁵ Department of Mechanical Engineering, Nan Kai Institute of Technology, Nantou 54243, Taiwan

E-mail: srjian@gmail.com

Received 4 April 2006, in final form 19 June 2006

Published 6 July 2006

Online at stacks.iop.org/Nano/17/3838

Abstract

The nanometre-scale oxidation characteristics of a p-GaAs(100) surface are investigated by atomic force microscope (AFM) electrochemical nanolithography with a multiwalled carbon nanotube (MWCNT) probe. The electrochemical parameters, such as anodizing voltages, scanning rate and modulated voltages, and how they affect the creation and growth of the oxide nanostructures are explored. The present results reveal that the initial growth rate ($\sim 600 \text{ nm s}^{-1}$ for 10 V) decreases rapidly as the electric field strength is decreased. The oxide practically ceases to grow as the electric field is reduced to the order of $\sim 1.2 \times 10^7 \text{ V cm}^{-1}$. Also, the oxide growth rate depends not only on the electric field strength but also on the applied anodizing voltage. The present results show that the height of the oxide structures can be significantly improved at an applied anodizing voltage of 10 V by using a CNT probe. In addition, Auger electron spectroscopy (AES) measurements performed in the present work confirm that modified structures replace the form of anodizing p-GaAs(100).

(Some figures in this article are in colour only in the electronic version)

1. Introduction

While scanning probe microscopy (SPM) has been shown to be a powerful tool for modifying various surfaces at the nanometre-scale [1], lithographic methods using an atomic force microscopy (AFM)-based local anodic oxidation process have been investigated for the fabrication of nanostructures [2] and nanodevices such as single electron transistors [3], Josephson junctions and superconducting

quantum interference devices (SQUIDS) [4]. In addition, the parallel writing technique based on arrays of AFM probes has been recently developed [5, 6] for industrial mass production of nanodevices. However, to adopt the oxide dots and wires successfully as integral parts of nanodevices serving as effective tunnel barriers for carrier transport, further improvements/enhancements of the aspect ratios of oxide structures are needed.

The size of the oxide structure fabricated by the techniques mentioned above is significantly determined by the probe

⁶ Author to whom any correspondence should be addressed.

apex; therefore the use of carbon nanotubes (CNTs) as tips in AFM was suggested in [7] as an effective way to decrease the probe apex. CNTs have been suggested as the ultimate high-resolution probe for AFM [8] because of their excellent characteristics, such as the high aspect ratio that provides the ability to probe deep crevices and steep features, the small tip radii of curvature (less than 10 nm), and excellent mechanical robustness and electrical conductivity, which provide great advantages for imaging and lithography tools with respect to conventional Si or Si₃N₄-based probes (with a tip radius of curvature of 10 nm or much larger). CNTs have actually been found to be useful and have a prolonged life time in imaging material surface structures at greater depths and softnesses owing to their unique mechanical, electronic and chemical characteristics. In addition, CNTs have considerable mechanical flexibility and thus can be elastically buckled without damage [8, 9]. Therefore, nanotube-attached probes are robust and will not be broken off by accidentally crashing onto a sample surface, whereas conventional scanning probes are easily chipped.

In this study, we performed AFM-based local anodic oxidation on a p-GaAs(100) surface with multiwalled carbon nanotube (MWCNT) probes to fabricate the oxide structures under ambient conditions. We investigated how the electrochemical parameters (namely, the applied voltages, the scanning rates and the modulated voltages) influence the features of the oxide structures. In addition, micro-Auger analysis of the selectively oxidized region revealed the formation of Ga(As)O_x. Results herein indicate that the dimensions of the oxide structures can be improved by using CNT probes. As shown in this work, AFM nanolithography with CNT probes is a promising method for fabricating very small oxide structures and therefore has great potential for use in the fabrication of future nanodevices.

2. Experimental details

In this study, nanolithography was carried out by means of a commercial AFM (NT-MDT Solver-P47, Russia) in the non-contact mode (ncAFM) at room temperature with a humidity of 55%. A modified cantilever (Daiken-Kagaku, 3 N m⁻¹, 157 kHz) with a conductive MWCNT (~10 nm in diameter and ~300 nm in length) on the Si probe was employed for imaging and nano-oxidation. The sample was p-GaAs(100) with a resistivity of 10 Ω cm, and with a root-mean-square surface roughness of less than 0.25 nm.

By the application of a bias voltage between the sample surface and the AFM CNT probe, the oxide structures were grown on the electrochemically reactive surface. For anodization of oxide dots, the applied anodizing voltages were varied between 8 and 10 V and the pulse duration ranged from 0.001 to 100 s, acting on various surface positions through the AFM CNT probe. For anodization of oxide wires, the effects of various scanning rates ranging from 0.1 to 10 μm s⁻¹ at anodizing voltages of 8 and 10 V were investigated. For the voltage modulation studies, an AC voltage was applied to the AFM CNT probe; the high level and low level of the voltage amplitude were 10 and -10 V, respectively, and their corresponding pulse durations were 50 ms, compared with a

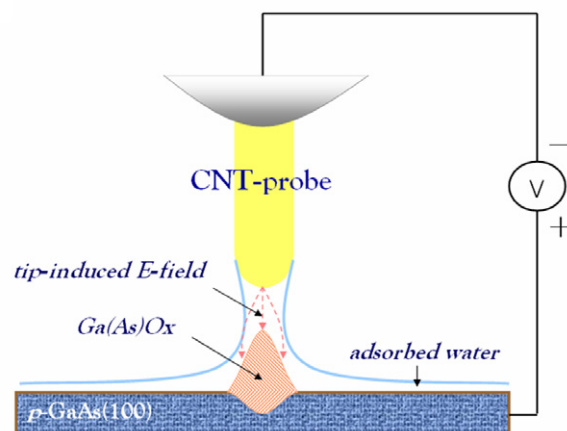


Figure 1. Schematic drawing of nano-oxidation using a CNT probe.

DC voltage. The presented data are an average of the five experiments.

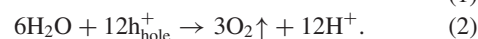
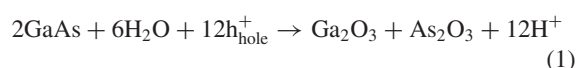
To investigate the conversion of GaAs oxides, the chemical composition of the sample was analysed by an Auger electron spectroscopy (AES; Auger 670 PHI Xi, Physical Electronics, USA) system equipped with a Schottky field emission electron source.

3. Results and discussion

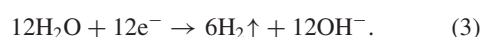
The mechanism of anodic oxidation on the p-GaAs(100) surface by ncAFM with a MWCNT probe is depicted in figure 1. When an AFM probe is brought to a sample surface in humid air, a water bridge is formed around the tip-sample junction due to the capillary force. The AFM probe acts as a cathodically biased electrode at the sample surface, while the layer of adsorbed water on the sample surface dissociates owing to a high electric field and acts as an electrolyte producing this electrochemical reaction. Oxyanions (OH⁻ and O⁻) contribute to the formation of the surface oxides and, owing to diffusion through the oxide layer, also to the growth of oxides underneath.

The oxide protrudes out of the GaAs surface because of the volume expansion as a result of the incorporation of the oxygen atoms. The chemical reactions and charge transfer processes have to be generally considered while analysing the kinetics of anodic oxidation on the p-GaAs(100) surface, as follows:

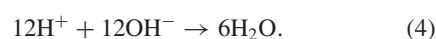
- (i) Reactions at the p-GaAs(100) surface:



- (ii) Reaction at an AFM probe:



- (iii) Reaction in water:



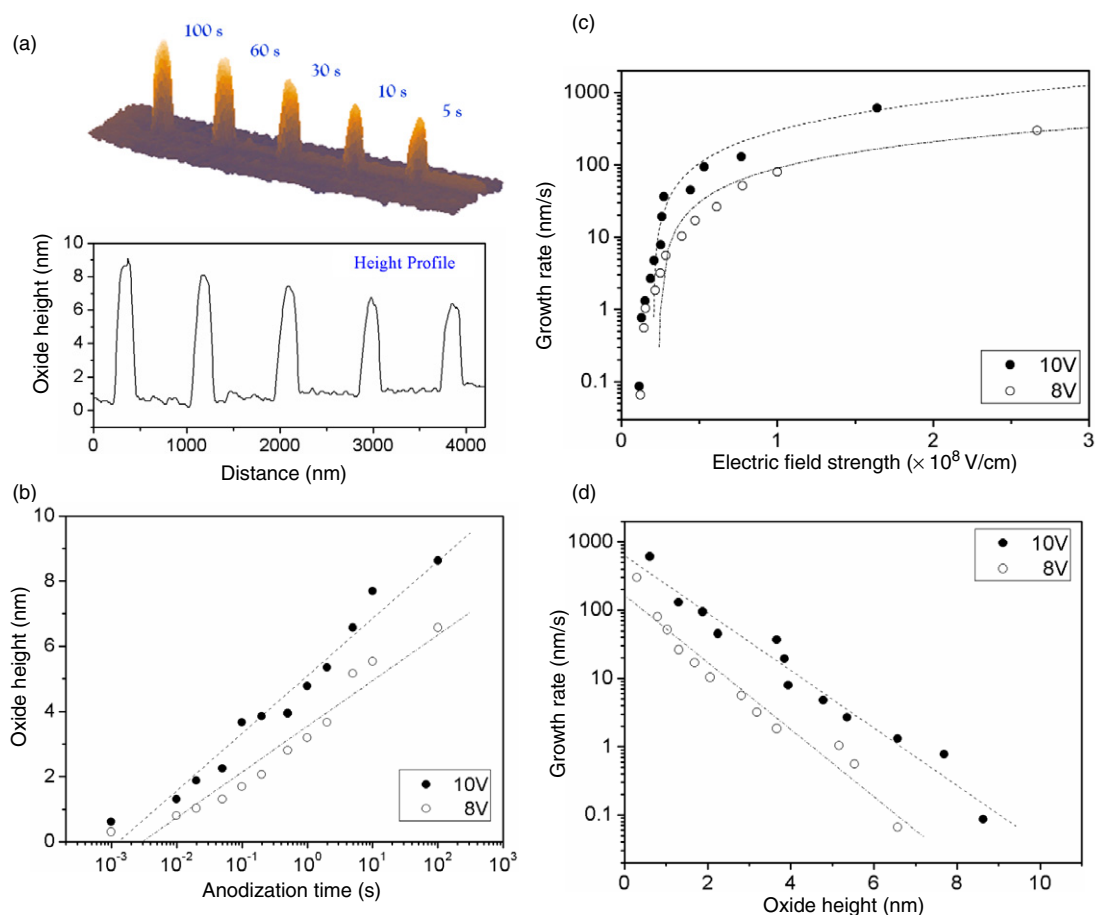


Figure 2. (a) An AFM image displaying a series of point oxide protrusions, from right to left, which are obtained at anodizing pulses of 10 V of 5, 10, 30, 60 and 100 s, respectively, and the corresponding height profile. (b) Oxide height as a function of the anodization time at two different voltages. (c) Relationship of the growth rate and the electric field strength. (d) Oxide height versus growth rate.

In the case of nano-oxidation, therefore, it can be expected that the H^+ and OH^- ions generated by reactions (1)–(3) will recombine immediately according to the recombination reaction (4). Here, h_{hole}^+ denotes positively charged holes on the p-GaAs(100) surface.

Figure 2(a) shows an AFM image in which a series of point oxide protrusions, from right to left, are produced via 10 V pulses of 5, 10, 30, 60 and 100 s, respectively. It can be seen that the average full width at half maximum of the point oxide protrusions is ~ 200 nm, and the height of the protruded point oxide increases concurrently with pulse time. This indicates that oxide growth follows the direction (perpendicular to the surface) of the electric field with time. Notably, this experimental result is similar to those presented previously [10] regarding anodization at varying static voltages and pulses for the duration.

Kinetic measurements are shown in figure 2(b) where the height of the oxide dots is plotted as a function of the anodization time. For advanced study of the oxidation kinetics, further analyses are discussed below. From figure 2(b), we can estimate the oxide height to which the electrochemical process is diffusion limited as ~ 9 nm, and can obtain the growth rate as a function of electric field strength as shown in figure 2(c). The initial growth rate is of the order of ~ 600 nm s^{-1} for 10 V and it decreases exponentially with decreasing field

strength. Also, it was found that the anodization process is enhanced when the electric field strength is of the order of $\sim 1.2 \times 10^7$ V cm^{-1} . In figure 2(c), not only is the growth rate a function of electric field strength but it also appears to depend on the applied anodizing voltage. In 1997, Avouris *et al* [10] proposed that the growth kinetics can be described as $dh/dt \propto \exp(-h/l_c)$, where h is the oxide thickness at time t and l_c is a characteristic decay length depending on the anodization voltage. Figure 2(d) displays the relationships between the growth rate and the oxide height at two different applied bias voltages. The characteristic decay length l_c is 0.88 and 1.03 nm at applied anodizing voltages of 8 and 10 V, respectively.

The ncAFM anodization was subjected locally to two different voltages; the diffusion limited electric field strength corresponding to the oxide height of ~ 9 nm for 10 V is $\sim 1.2 \times 10^7$ V cm^{-1} . An oxide protrusion of greater height corresponds to a weaker electrical field strength, which limits the growth of the oxide structures. The growth rate of the anodizing surface is governed by the ionic transportation promoted by the electric field strength. This accounted for the self-limiting growth, which was proposed by Stiévenard *et al* [11]. The growth of the oxide structure is therefore fast in the initial stage of the anodization process while there is a simultaneous rapid buildup of the space charge. Obviously, the applied voltage extends

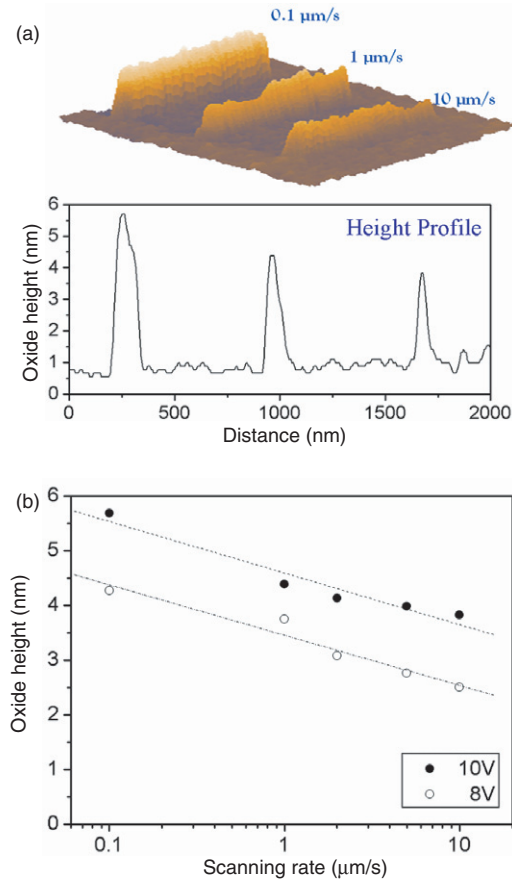


Figure 3. (a) An AFM image and the height profile of GaAs oxide wires patterned using a scanning rate of 0.1, 1 and 10 $\mu\text{m s}^{-1}$ at an anodizing voltage of 10 V, respectively. (b) The effects of the scanning rate and applied voltage on the height of the oxide wire structure.

the electric field strength, assisting the oxidation mechanisms until the growth is limited by the diffusion. It is evident that the simple Cabrera–Mott model [12] of field-induced oxidation cannot account for the observed kinetics. The possible differences between the kinetics of AFM nano-oxidation and the Cabrera–Mott field model have been attributed to the following mechanisms: (1) the mechanical stress created and arising within the oxide dots due to a large volume of mismatch between the sample and the oxides [13] and (2) build-up of the space charge within the oxide dots [14].

Furthermore, compared with our previous study [2], the present work shows that the height of the oxide protrusions can be improved by $\sim 50\%$ and the initial growth rate can be doubled at an applied anodizing voltage of 10 V by using a CNT as the AFM probe.

Besides dot patterns, an oxide wire pattern was also fabricated. The wires were formed with scanning rates of 0.1, 1 and 10 $\mu\text{m s}^{-1}$ at anodizing voltages of 10 V, as shown in figure 3(a). Figure 3(b) shows the relationship between the scanning rate of the AFM probe and the height of the oxide wire. With an increase in the scanning rate from 0.1 to 10 $\mu\text{m s}^{-1}$, the height and the width of the anodizing wire decreased. In other words, the faster the scanning rate the smaller the anodizing oxide structure. In terms of the oxidation

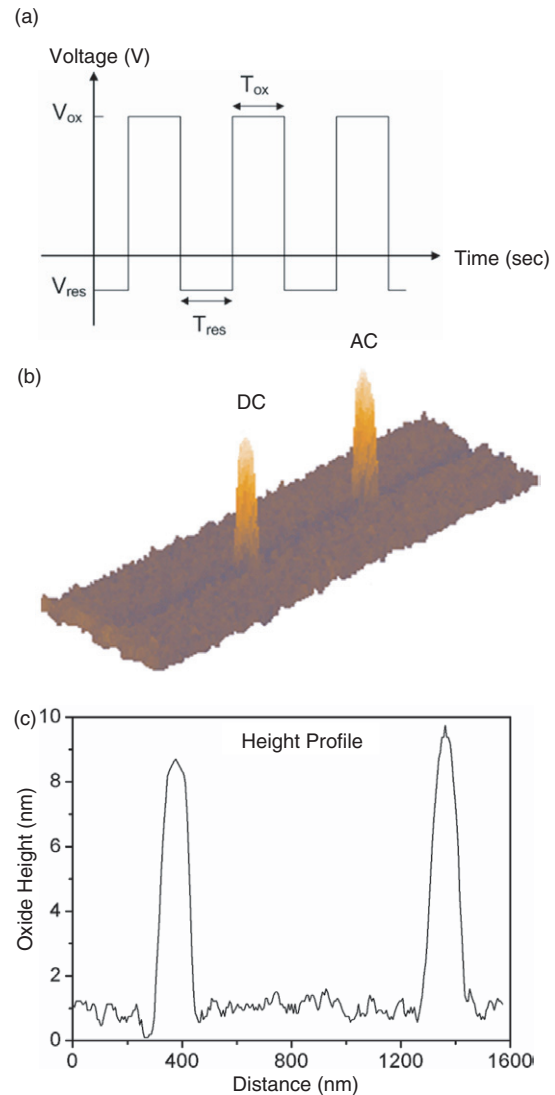


Figure 4. (a) Waveform voltage applied to the GaAs surface with respect to the CNT probe when performing an oxidation under AC conditions: T_{ox} is the time for which the oxidation is performed (the voltage applied to the sample is V_{ox}), and T_{res} is the rest time (the voltage applied is V_{res}). (b) An AFM image representation of two fabricated dots, left (DC voltage of 10 V and total time = 30 s) and right (AC voltage, $T_{\text{ox}} = T_{\text{res}} = 50$ ms, $V_{\text{ox}} = 10$ V, $V_{\text{res}} = -10$ V and total time = 60 s), at a relative humidity of 55%. (c) The height profile of two oxide dots, showing that the increase in height occurs at the central part of the dot by applying an AC voltage.

of silicon, it has been reported that the height of the oxidized area varies with scanning rate (v) of the AFM probe and is proportional to $\log(1/v)$ [10], $v^{-1/2}$ [15] and $v^{-1/4}$ [16] for a given bias. In this work, the height of the p-GaAs oxide wire pattern was found to be proportional to $\log(1/v)$ as illustrated in figure 3(b). Furthermore, the values for AFM-induced oxide wires on n^+ -GaAs(100) surface [13] (ranging from 2 to 4 nm at 10 V) are less than our present results.

To investigate the effect of modulated voltages on the fabrication of the oxide protrusions, the operation of AC and DC voltages is discussed next.

The parameters defining the AC square waveform are illustrated in figure 4(a). The waveform consists of a series of

pulses where T_{ox} and T_{res} are denoted as the oxidation time and the rest time; V_{ox} and V_{res} are applied voltages during T_{ox} and T_{res} , respectively. We refer to $1/(T_{\text{ox}} + T_{\text{res}})$ as the frequency of the waveform. The total oxidation time is T_{ox} multiplied by the number of pulses. In figure 4(b), two oxide dots were grown by applying AC and DC voltages, respectively.

The electrochemical oxidation process is a source of hydrogen species. The neutralization reaction, equation (4), becomes significant while the proton concentration increases after a long anodization time. As less OH^- arrives at the GaAs/Ga(As) O_x interface, the rate of growth of (the height of) the oxide would be decreased. Meanwhile, lateral diffusion of OH^- at the water/oxide interface gradually becomes significant and, therefore, the width of the oxide increases. Nevertheless, this phenomenon can be halted by applying an AC voltage with the negative rest voltages. During the rest time T_{res} , H^+ ions will be removed from the GaAs/Ga(As) O_x interface and the transport of OH^- interrupted. It has been verified that the application of V_{res} cannot produce any appreciable oxidation on the surface. Until the next voltage pulse is activated at V_{ox} , the directional transport of OH^- will be restarted and the vertical growth of the oxide dot will continue. Therefore, a shaper structure can be obtained under AC conditions at the central part of the dot where the electric field strength is supposed to be higher. Compared with the dot fabricated by DC voltages, the increased ratio of the height is ~ 1.1 , as shown in figure 4(c). The same tendency for the oxides height to be enhanced under AC conditions can be found in previous studies [17, 18]. In addition, the oxide dots grown by a CNT probe are much higher.

On the other hand, it is interesting to note that the base width of two oxide dots is almost the same. As pointed out by Calleja *et al* [18], the modulated frequency is an important factor determining the geometric dimension of the oxide protrusions. The lateral diffusion can be greatly suppressed at higher frequencies (> 100 Hz), resulting in a narrower oxide base. There is no obvious lateral diffusion in our present work ($f = 10$ Hz). The main reason is that centralization of the electric field using a CNT probe results in the ion transport strongly following the direction of the electric field during the AC process. In summary, the application of an AC voltage to induce the oxidation significantly modifies the higher aspect ratio of oxide protrusions compared with the DC condition.

According to the above-mentioned statements, no matter what the oxide structures or applied voltage are, much higher oxide protrusions are obtained by using a CNT probe than a conventional one. We deduced that the smaller apex of the CNT probe means that the water bridge is narrower, resulting in centralization of the electric field and further enhancement of the oxidation process. In addition, from the report of Teuschler *et al* [16], p-type Si(111):H has a higher oxide height than that of the n-type at a particular applied voltage, as well as a higher growth rate. Thereby, we can reasonably deduce that the difference is attributed to the differently doped substrates, the geometric shape of probe and operational conditions (such as AFM-operated mode, the humidity, etc).

In order to investigate the chemical composition of the anodizing structures, AES analysis was conducted on an anodizing area of $10 \times 10 \mu\text{m}^2$ (5–6 nm oxide height). The Auger spectra taken from the as-grown and modified areas are

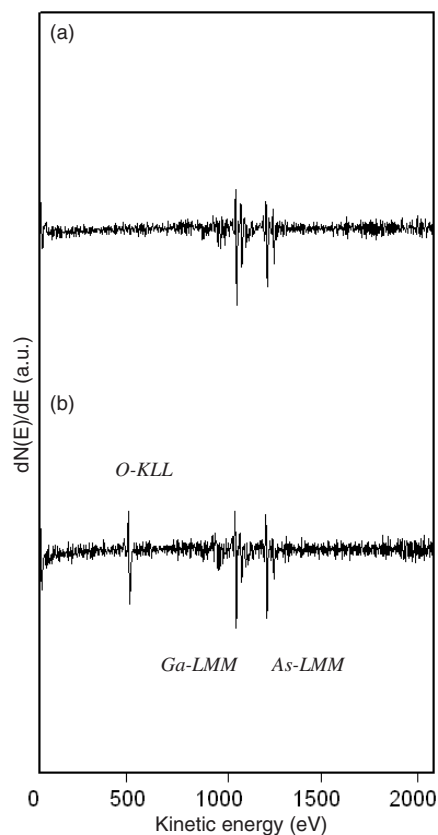


Figure 5. AES spectra of (a) the as-grown and (b) the anodizing oxide areas on the p-GaAs(100) surface.

illustrated in figure 5. Both spectra have emission peaks of Ga-LMM at ~ 1065 eV and As-LMM at ~ 1225 eV. Obviously, we can see the emission peak of O-KLL Auger electrons having a kinetic energy of ~ 512 eV in figure 5(b). Meanwhile, the magnitude of O-KLL is much enhanced on the anodizing region as compared to that of the as-grown region, which suggests higher oxygen content in GaAs owing to AFM nano-oxidation, resulting in the formation of anodizing GaAs. AES results also support the suggestion of the previous study [19] that the heavily C-doped GaAs film can be converted to oxides by a local oxidation process: mobile oxyanions drift toward the anodic sample in response to the local electrical field beneath an AFM tip and react with the p-GaAs(100) surface at the oxide/GaAs interface. On the other hand, x-ray photoelectron spectroscopy (XPS) is also a powerful technique for analysing surface chemistry and composition. The chemical analysis of AFM tip-induced n⁺-GaAs(100) oxides using scanning microprobe XPS measurements [20] has also revealed that the main constituents are Ga₂O₃ and As₂O₃. In view of AES and XPS analysis, the products are shown to be GaAs oxides in a qualitative analysis briefly.

4. Conclusion

In summary, the oxidation characteristics of p-GaAs(100) have been successfully demonstrated by AFM electrochemical nanolithography with an attached MWCNT probe. In this electrochemical reaction, the chemical composition of the

selectively oxidized GaAs area was determined by micro-Auger analysis. Results revealed that the local anodic oxidation process is enhanced at electric field strengths of the order of $\sim 1.2 \times 10^7 \text{ V cm}^{-1}$. In addition, the higher the oxide protrusions the weaker the electric field strength becomes, which limited the growth of the oxide protrusions. It is found that the oxide wire increases linearly with applied anodizing voltage and decreases logarithmically with scanning rate. Also, the height of the oxide wires was found to be proportional to $\log(1/v)$. On the other hand, the application of an AC voltage to induce the oxidation significantly modifies the aspect ratio of the oxide protrusions.

Acknowledgments

This work was partially supported by the National Science Council of Taiwan, under grant nos: NSC94-2112-M-002-002, NSC94-2120-M-009-002, NSC94-2112-M-009-024, NSC89-2112-M-134-002, NSC90-2112-M-134-002, NSC91-2112-M-134-001 and NSC92-2112-M-134-001.

References

- [1] Snow E S, Campbell P M and Perkins F K 1997 *Proc. IEEE* **85** 601
- [2] Jian S R, Fang T H and Chuu D S 2005 *J. Phys. D: Appl. Phys.* **38** 2424
- [3] Matsumoto K 1997 *Proc. IEEE* **85** 612
- [4] Bouchiat V, Faucher M, Thirion C, Wernsdorfer W, Fournier T and Pannetier B 2001 *Appl. Phys. Lett.* **79** 123
- [5] Cavallini M, Mei P, Biscarini F and García R 2003 *Appl. Phys. Lett.* **83** 5286
- [6] Kakushima K, Watanabe T, Shimamoto K, Gouda T, Ataka M, Mimura H, Isono Y, Hashiguchi G, Mihara Y and Fujita H 2004 *Japan. J. Appl. Phys.* **43** 4041
- [7] Iijima S 1991 *Nature* **354** 56
- [8] Dai H, Hafner J H, Rinzler A G, Colber D T and Smalley R E 1996 *Nature* **387** 147
- [9] Wong E W, Sheehan P E and Lieber C M 1997 *Science* **277** 1971
- [10] Avouris Ph, Hertel T and Martel R 1997 *Appl. Phys. Lett.* **71** 285
- [11] Stiévenard D, Fontaine P A and Dubois E 1997 *Appl. Phys. Lett.* **70** 3272
- [12] Cabrera N and Mott N F 1949 *Rep. Prog. Phys.* **12** 163
- [13] Okada Y, Amano S, Kawabe M and Harris J S Jr 1998 *J. Appl. Phys.* **83** 7998
- [14] Dagata J A, Inoue T, Itoh J, Matsumoto K and Yokoyama H 1998 *J. Appl. Phys.* **84** 6891
- [15] Yasutake M, Ejiri Y and Hattori T 1993 *Japan. J. Appl. Phys.* **32** L1021
- [16] Teuschler T, Mahr K, Miyazaki S, Hundhausen M and Ley L 1995 *Appl. Phys. Lett.* **67** 3144
- [17] Okada Y, Iuchi Y and Kawabe M 2000 *J. Appl. Phys.* **87** 8754
- [18] Calleja M, Anguita J, García R, Birkelund K, Pérez-Murano F and Dagata J A 1999 *Nanotechnology* **10** 34
- [19] Shirakashi J I, Matsumoto K and Konagai M 1998 *Appl. Phys. A* **66** S1083
- [20] Okada Y, Iuchi Y, Kawabe M and Harris J S Jr 1998 *J. Appl. Phys.* **88** 1136